Cell Metabolism, Volume *25*

Supplemental Information

Obesity-Induced Metabolic Stress Leads to Biased Effector Memory $CD4^+$ T Cell Differentiation via PI3K p110δ-Akt-Mediated Signals

Claudio Mauro, Joanne Smith, Danilo Cucchi, David Coe, Hongmei Fu, Fabrizia Bonacina, Andrea Baragetti, Gaia Cermenati, Donatella Caruso, Nico Mitro, Alberico L. Catapano, Enrico Ammirati, Maria P. Longhi, Klaus Okkenhaug, Giuseppe D. Norata, and Federica M. Marelli-Berg

SUPPLEMENTAL INFORMATION

SUPPLEMENTAL EXPERIMENTAL PROCEDURES

Determination of abdominal adiposity (android/gynoid ratio)

Total body DXA scans were acquired using Lunar iDXA (GE Healthcare, Madison, WI). Daily quality control scans were acquired during the study period. All subjects were scanned while wearing a hospital gown with all metal artifacts removed from their body. Trained operators, blinded on patient's identity and clinical history, performed all scans. Patient positioning and data acquisition was conducted in accordance to the operator's manual. Lunar iDXA scans were analyzed with the enCORE software (version 14.0), (GE Healthcare, Madison, WI), (Rothney et al., 2013). Out of total weight, the software allows to discriminate the bone mass, the fat mass and the lean mass. DXA android fat was computed automatically over the DXA android region, a region-of-interest automatically defined by the enCORE software, whose caudal limit is automatically placed at the top of the iliac crest and whose height is set to 20% of the distance from the top of the iliac crest to the base of the skull to define its cephalad limit. DEXA gynoid fat was computed automatically as well, over the DXA gynoid region (percent of fat tissue in inferior half abdominal, glutei and femoral regions); their ratio is automatically determined by the software to give the gender-adjusted measure of abdominal obesity (Rothney et al., 2013).

Lipidomic profile by liquid chromatography-tandem mass spectrometry (LC-MS/MS)

All HPLC solvents were MS grade (Carlo Erba); fatty acid internal standards ^{13}C-labelled palmitic acid (C16:0) and ^{13}C-labelled linoleic acid (C18:2) were purchased from Sigma. Phospholipid standards: C13:0 lysophosphatidylcholines (LPC); C:25:0 phosphatidylcholines (PC); C12:0 sphingomyelin (SM); 12:0-13:0 phosphatidylserine (PS); 12:0-13:0 phosphatidylinositol (PI); 12:0-13:0 phosphatidylglycerol (PG); 12:0-13:0 phosphatidic acid (PA); 12:0-13:0 phosphatidylethanolamine (PE); C12 ceramide (Cer); glucosyl (β) C12 ceramide (GC); lactosyl (β) C12 ceramide (LacCer); C17 mono-sulfo galactosyl-(β)-ceramide (D18:1/17:0; GalCer); were purchased from Avanti Polar Lipids. Quantification of fifteen different fatty acids was performed as previously described (Cermenati et al., 2015). Briefly, samples were homogenized in methanol:acetonitrile (1:1). Aliquots of extracts, after addition of internal standards (^{13}C-labelled palmitic and linoleic acids), were subjected to acid hydrolysis and processed as previously described (Cermenati et al., 2015). Fatty acid quantification was performed on a API-4000 triple quadrupole mass spectrometer (AB Sciex) coupled with a HPLC system (Agilent) and CTC PAL HTS auto-sampler (PAL System) using standard curves for each fatty acid analyzed. For the quantification of the different phospholipids, the MS analysis was performed with a flow injection analysis-tandem mass spectrometry (FIA-MS/MS) method. The identity and quantification of the different phospholipids were confirmed using pure standards. Methanolic:acetonitrile extracts were analyzed by a 5 min run in both positive and negative ion mode with a 268 multiple reaction monitoring (MRM) transition in positive mode and 88 MRM transition in negative mode. An ESI source connected with an API 4000 triple quadrupole instrument (AB Sciex) was used. The mobile phase was 0.1 % formic acid in MeOH for FIA positive analysis and 5 mM ammonium acetate pH 7 in MeOH for FIA negative. MultiQuant™ software version 3.0.2 was used for data analysis and peak review of chromatograms. Each metabolite level detected was normalized on protein content.

SUPPLEMENTAL REFERENCES

Cermenati, G., Audano, M., Giatti, S., Carozzi, V., Porretta-Serapiglia, C., Pettinato, E., Ferri, C., D'Antonio, M., De Fabiani, E., Crestani, M.*, et al.* (2015). Lack of sterol regulatory element binding factor-1c imposes glial Fatty Acid utilization leading to peripheral neuropathy. Cell metabolism *21*, 571-583.

Rothney, M.P., Xia, Y., Wacker, W.K., Martin, F.P., Beaumont, M., Rezzi, S., Giusti, V., and Ergun, D.L. (2013). Precision of a new tool to measure visceral adipose tissue (VAT) using dual-energy X-Ray absorptiometry (DXA). Obesity (Silver Spring, Md.) *21*, E134-136.

SUPPLEMENTAL FIGURE AND TABLE LEGENDS

Supplemental Figure 1 (related to Figure 1). *In vivo* peritoneal recruitment and Rag2KO skin grafts. (A-B) Schematic of the design **(A)** and timeline **(B)** of the *in vivo* peritoneal recruitment model used in Fig 1A-D. **(C)** Weight gain curves of mice over the 8 weeks HFD or CD in C57Bl/6 male recipients and Marilyn female donors. **(D)** Survival curve of C57Bl/6 male skin grafts on HFD or CD Rag2KO female recipients up to 21 days post-transplantation. Also shown is the survival curve following reconstitution of HFD Rag2KO mice with $CD4^+$ T cells isolated from Marilyn female mice**. (C-D)** n=3-6 independent mice. **(C)** Values denote mean ± s.e.m. *P<0.05; **P<0.01.

Supplemental Figure 2 (related to Figure 2). HFD-induced differentiation of $CXCR3^+$-$LFA1^+$ effector memory-like phenotype in mice and *in vivo* sources of CXCL10. (A-F) Cell surface staining of CCR7 **(A)**, CD62L **(B)**, CXCR3 **(C)**, LFA1 **(D)**, CD25 **(E)** and CD44 **(F)**, in *in vivo*-primed $CD4^+$ T cells isolated from pooled lymph nodes of the HFD or CD Marilyn female donor mice used in Fig 1A-D (%). **(G)** Gating strategy defining immune cells tested for expression of CXCL10 in the peritoneal cavity 48 hours after *i.p.* injection of IFNγ (600U/mouse). **(H)** MFI of CXCL10 in the immune cell types defined in G. **(A-F)** n=3-6

independent donors. **(H)** n=2 independent mice. **(A-F)** Values denote mean ± s.e.m. *P<0.05; **P<0.01; *** P<0.001.

Supplemental Figure 3 (related to Figure 3). Flow cytometry gating strategy to identify CD4$^+$ T cell subsets in humans. Examples of the gating strategy used in an obese **(A)** and a lean **(B)** individual to identify the principal CD4$^+$ T cell subsets and some of the T cell subpopulations in the peripheral blood samples of lean, over-weight and obese subjects.

Supplemental Figure 4 (related to Figure 3). Body fat distribution association with inflammatory T cell subsets and inflammatory mediators. (A-B) Levels of CRP in the blood of lean, over-weight and obese subjects stratified according to BMI **(A)** and correlation of CRP with effector memory T cells **(B)**. **(C)** Body mass fat distribution of android and gynoid fat within a lean, overweight and obese individual (analysed with body composition by dual-energy X-ray absorptiometry, DEXA). **(D-E)** Correlation of HLADR$^+$ **(D)** and CCR5$^+$ effector memory T cells **(E)** with android/gynoid ratio. **(A-B, D-E)** n=187. ANCOVA, *P<0.05.

Supplemental Figure 5 (related to Figure 4). Dendritic cells from HFD-fed mice do not affect T cell differentiation. (A) Dot plots and quantification of *in vitro* proliferation of CFSE-labelled CD4$^+$ T cells isolated from pooled lymph nodes of CD Marilyn female mice incubated with CD11c$^+$ DC isolated from the spleen of HFD or CD C57Bl/6 male mice for 3 days. Undivided and 4th division populations are quantified by dilution of the CFSE-label. **(B)** Dot plots and quantification of *in vivo* proliferation of CFSE-labelled CD4$^+$ T cells isolated from pooled lymph nodes of CD Marilyn female *i.v.* injected into C57Bl/6 female recipient mice in combination with CD11c$^+$ dendritic cells isolated from the spleen of HFD or CD C57Bl/6 male mice *i.p.* injected for 5 days. Undivided, 1st and 2nd division populations are quantified from the spleen and mesenteric lymph nodes of recipient females by dilution of the CFSE-label. **(C)** Cell surface staining of CD44 and CCR7 in the population of CFSE-labelled CD4$^+$ T cells isolated *in vivo* from the spleen and mesenteric lymph nodes of the

C57Bl/6 recipient female mice. **(A)** n=3 independent mice (each mouse was tested in triplicate). **(B-C)** n=4 independent mice. Values denote mean ± s.e.m. *P<0.05; ** P<0.01; ***P<0.001.

Supplemental Figure 6 (related to Figures 5 and 6). Mechanistic insights in to saturated FA-induced effector memory differentiation of CD4$^+$ T cells. (A) Levels and densitometric quantification of p-Akt (T308), Akt, p-S6 (S235/236) and S6 protein expression in *in vivo*-primed CD4$^+$ T cells isolated from mesenteric lymph nodes of CD and HFD mice *i.p.* injected with the PI3K inhibitor IC87114 or left untreated. **(B)** Volcano plot of fatty acids and phospholipids detected in in *in vivo*-primed CD4$^+$ T cells isolated from mesenteric lymph nodes of CD and HFD mice. Fifteen fatty acids were detected including palmitic acid C16:0; palmitoleic acid C16:1; margaric acid C17:0; stearic acid C18:0; oleic acid C18:1; linoleic acid C18:2; γ-linolenic acid C18:3; arachic acid C20:0; arachidonic acid C20:4; eicosapentaenoic acid C20:5 (EPA); behenic acid C22:0; erucic acid C22:1; docosahexaenoic acid C22:6 (DHA); lignoceric acid C24:0; nervonic acid C24:1. Out of 356 phospholipids analyzed (including LysoPC: lysophosphatidylcholine; PC: phosphatidylcholine; PC aa: phosphatidylcholine acyl-acyl; PC ae: phosphatidylcholine acyl-alkyl also known as plasmalogens; PE: phosphatidylethanolamine; PE aa: phosphatidylethanolamine acyl-acyl; PE ae: phosphatidylethanolamine acyl-alkyl also known as plasmalogens; PS: phosphatidylserines; LysoPI: lysophosphatidylinositol; PI: phosphatidylinositol; PG: phosphatidylglycerol; LysoPA: lysophosphatidic acid; PA: phosphatidic acid; SM: sphingomyelin; Cer: ceramide; GCer: glucosyl/galactosyl-ceramide; LacCer: lactosyl-ceramide and gangliosides GM1, GM2 and GM3) 229 different species belonging to different families were detected. The volcano plot displays the relationship between fold-change (expressed as log2) and significance between the two groups (CD vs. HFD), using a scatter plot view. The y-axis is the negative log10 of p values (a higher value indicates greater significance as indicated by dashed lines) and the x-axis is the difference in levels of metabolites between two experimental groups. Significantly increased metabolites

are shown by blue dots while red dots represented those decreased. **(C)** Representative fluorescence images of the aggregation of CTxB signal. **(D)** Levels and densitometric quantification of p-Akt (S473) and Akt protein expression in $CD4^+$ T cells isolated from pooled lymph nodes of mice, then activated with plate bound anti-CD3 (0.5µg/ml, ebioscience) and anti-CD28 (2.5µg/ml, ebioscience) for 6hrs in the presence or absence of the Akt activator SC79 (500 nM). **(E)** Levels and densitometric quantification of p-Akt (T308) and Akt protein expression in *in vivo*-primed $CD4^+$ T cells isolated from mesenteric lymph nodes of CD mice *i.p.* injected with the Akt activator SC79 or left untreated. **(A, D-E)** Each lane shows data from independent mouse samples. **(B)** n=3 independent mice. Values denote mean ± s.e.m. *P<0.05; **P<0.01.

Supplemental Table 1 (related to Figure 3). Parameters analysed in the n=1,172 subjects selected. All the variables were non-normally distributed (Kolmogorov-Smirnov test). Median (Interquartile-Range, IQR) are presented for each variable across subjects divided into lean (BMI< 25 Kg/m^2), overweight (BMI≥ 25 Kg/m^2) and obese (BMI < 30 Kg/m^2). Grubb's test was performed for detection of outliers (below and above 1.5∗IQR) for each distribution. P is derived from Analysis of covariance (ANCOVA) adjusting for age, gender and therapies.

Supplemental Table 2 (related to Figures 1, 2 and 4-7). Nutrients and caloric composition of diets: HFD, CD, PED and PCD.

Supplemental Figure 1 (related to Figure 1)

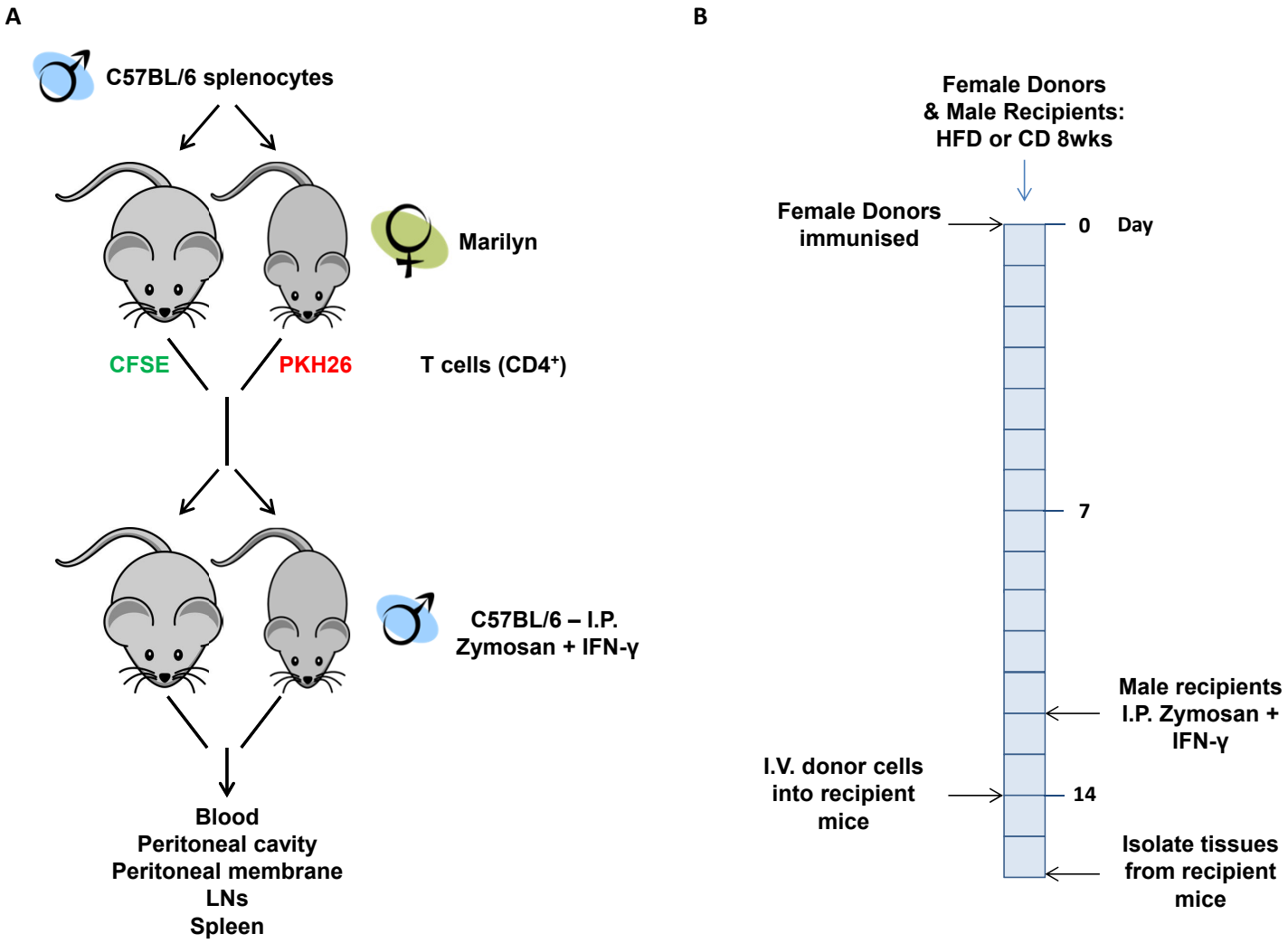

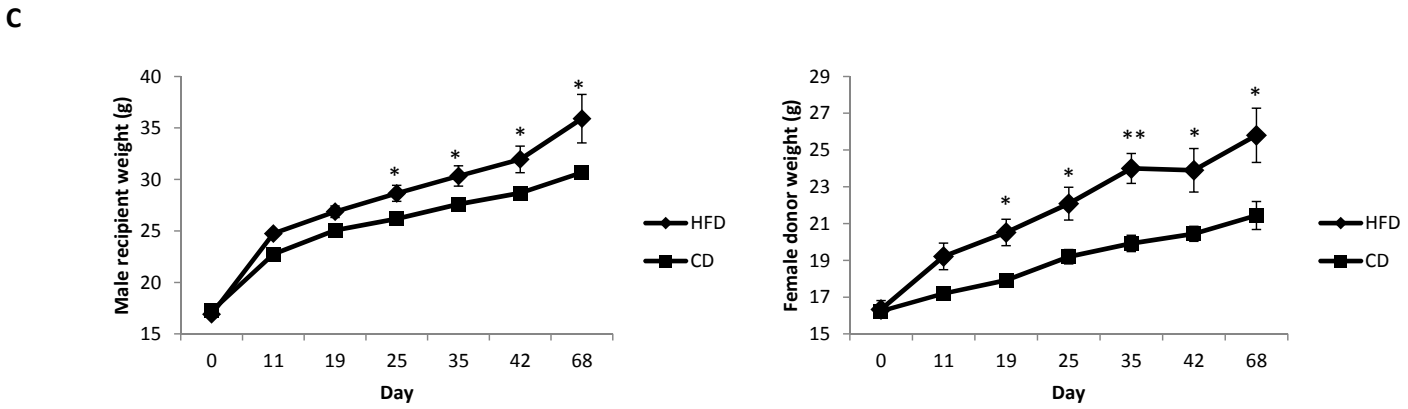

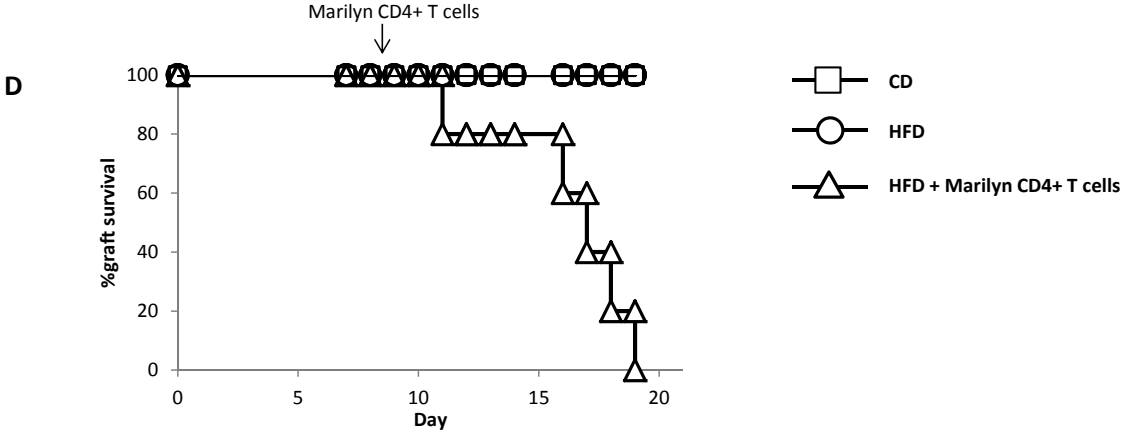

Supplemental Figure 2 (related to Figure 2)

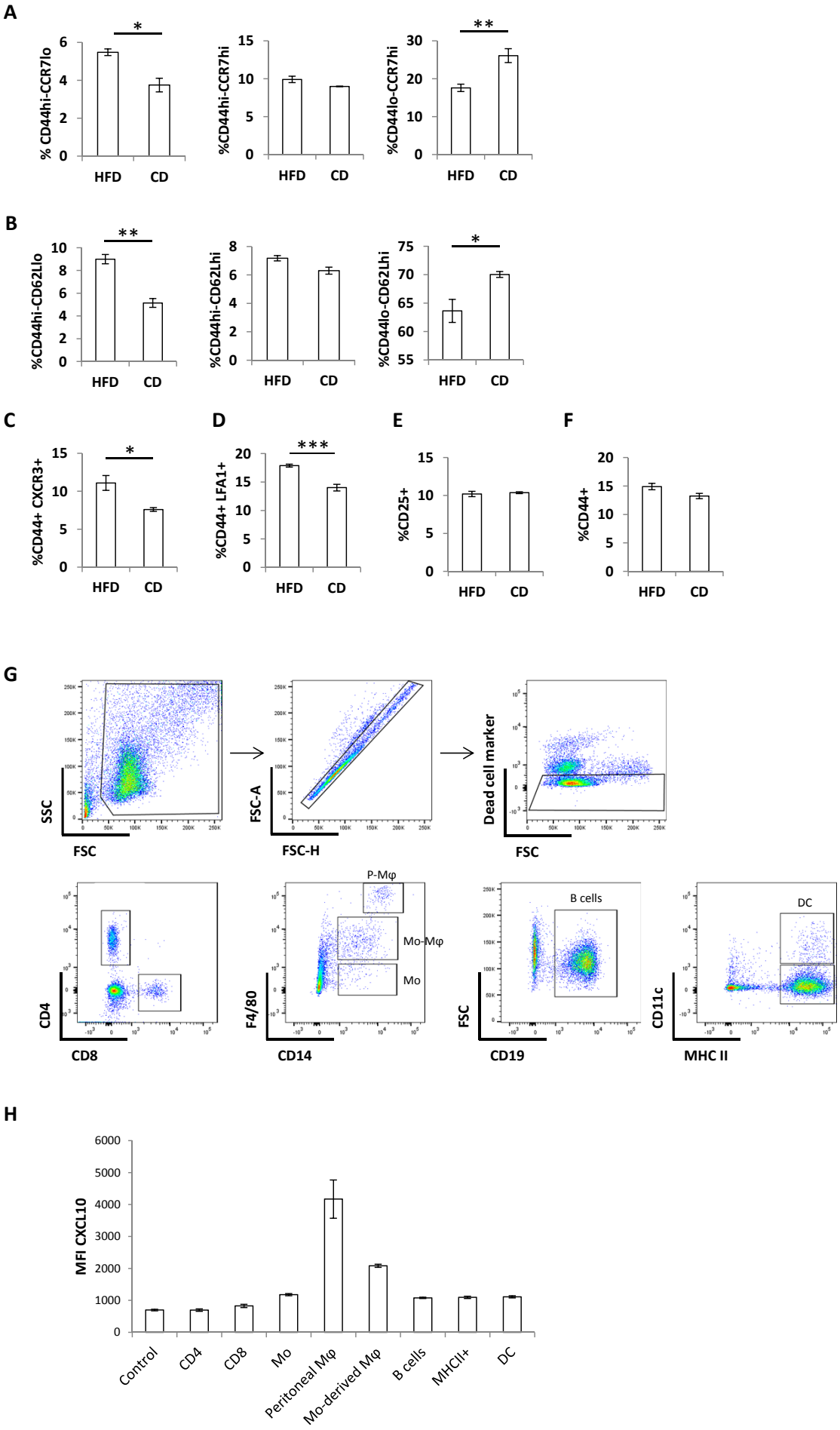

Supplemental Figure 3 (related to Figure 3)

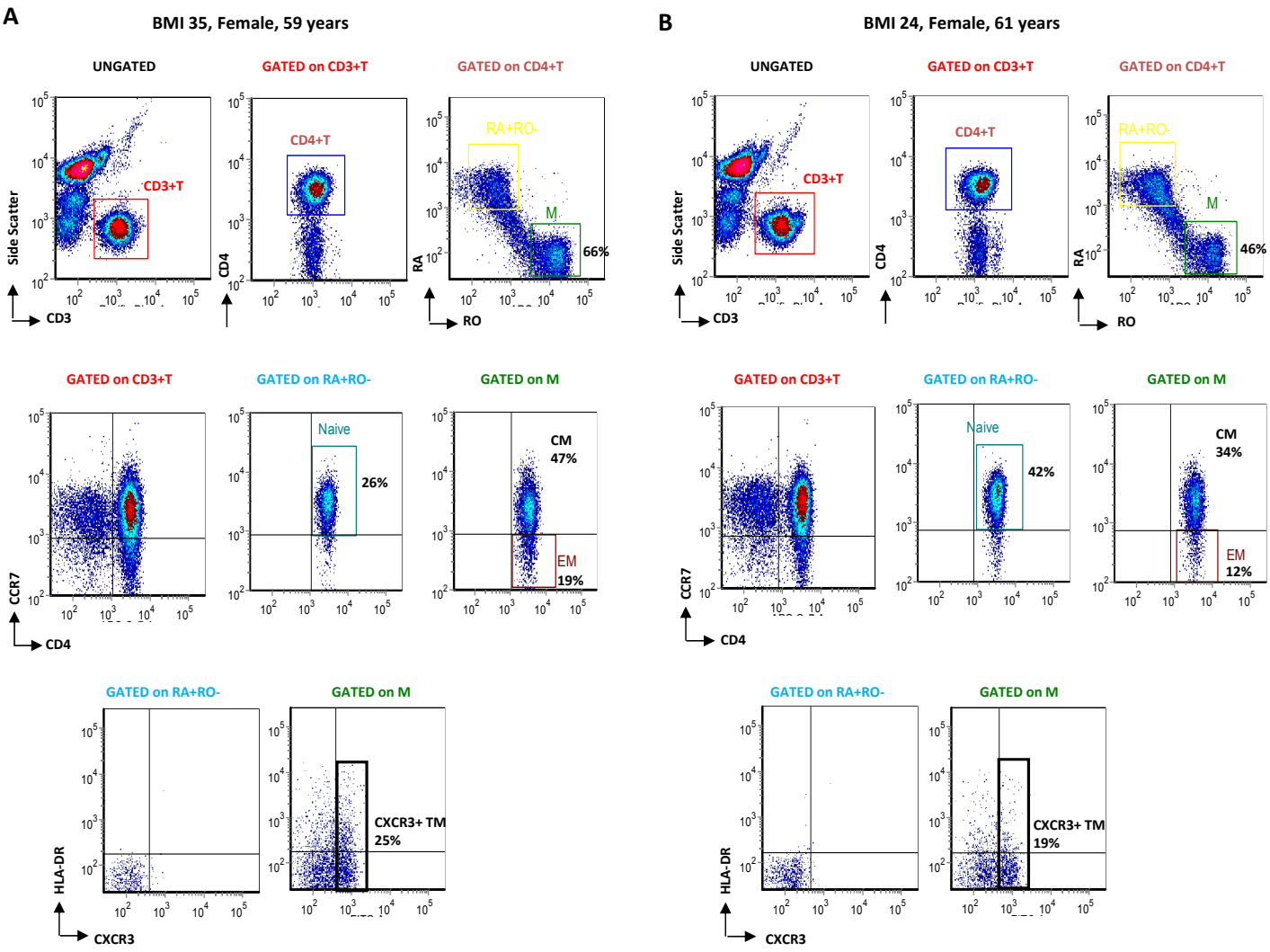

Supplemental Figure 4 (related to Figure 3)

A

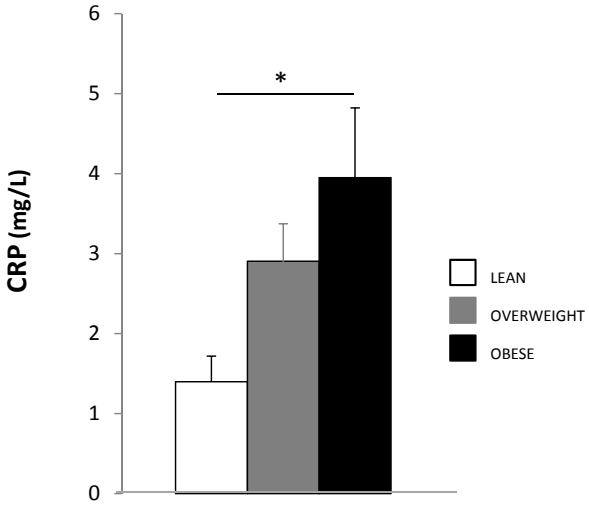

B

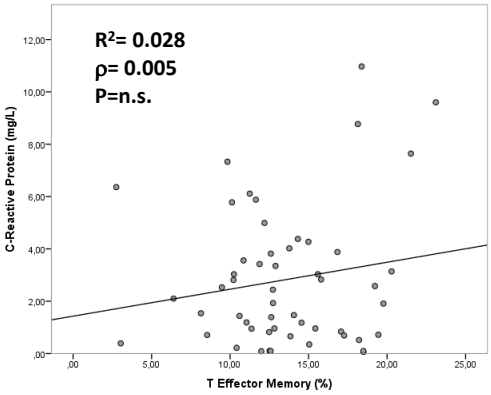

C

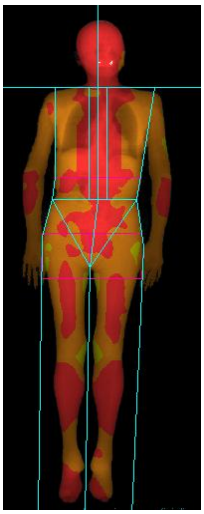

LEAN

Female 66 years
BMI: 19.2 Kg/m²
Android fat: 25.2%
Gynoid fat: 36.4 %
A/G_r : 0.69

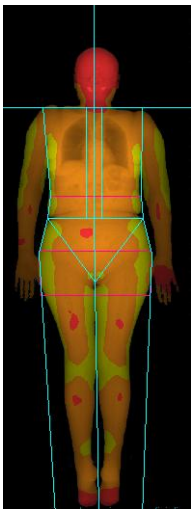

OVERWEIGHT

Female 66 years
BMI: 26.2 Kg/m²
Android fat: 51.2%
Gynoid fat: 54.3 %
A/G_r : 0.94

OBESE

Female 66 years
BMI: 37.8 Kg/m²
Android fat: 63.4%
Gynoid fat: 52.4 %
A/G_r : 1.21

D

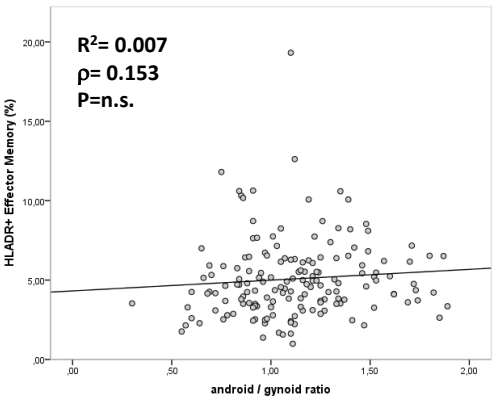

E

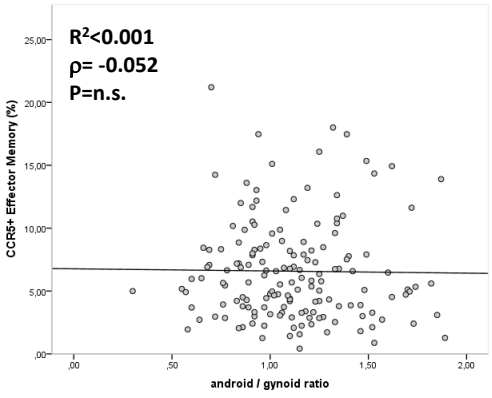

Supplemental Figure 5 (related to Figure 4)

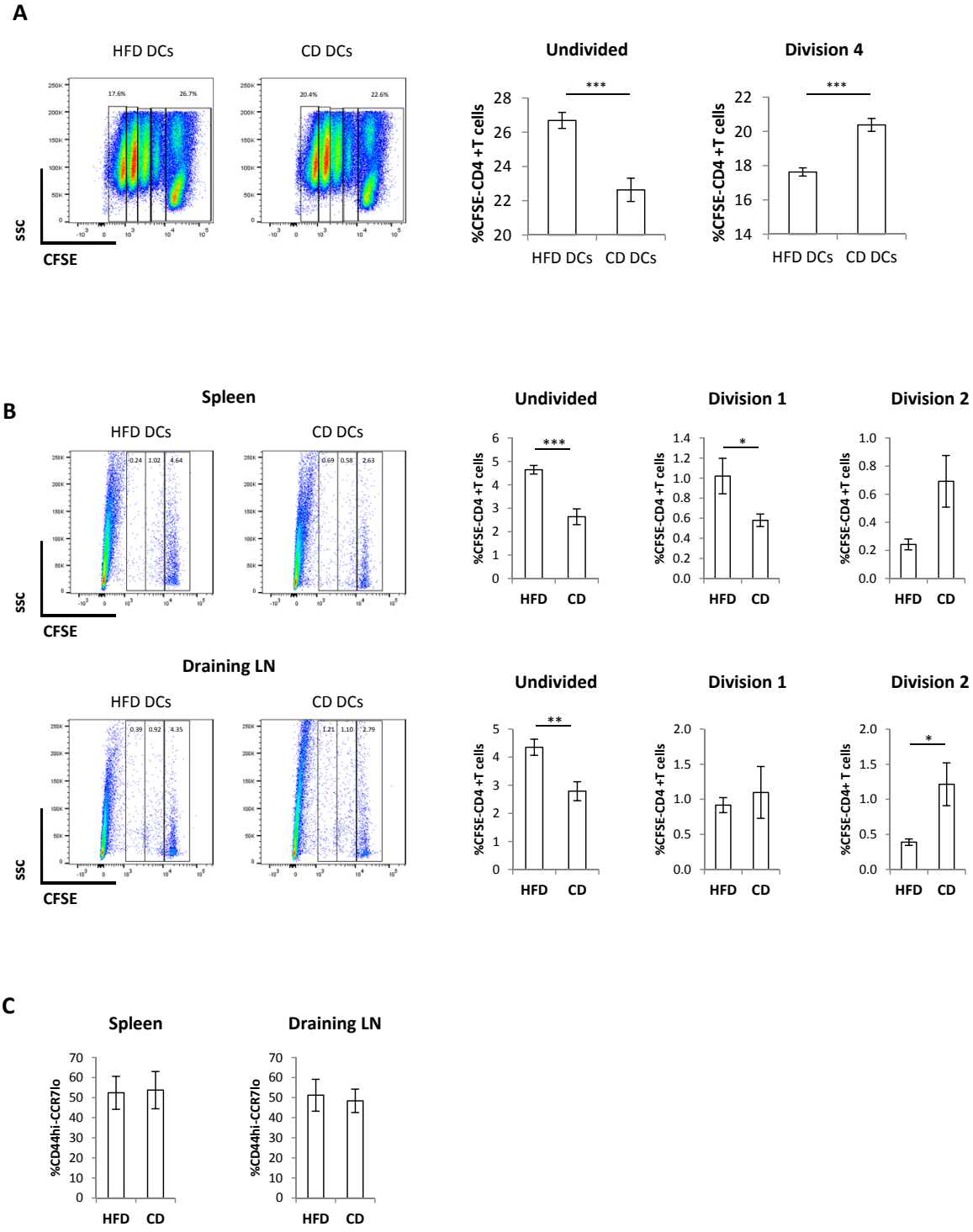

Supplemental Figure 6 (related to Figures 5 and 6)

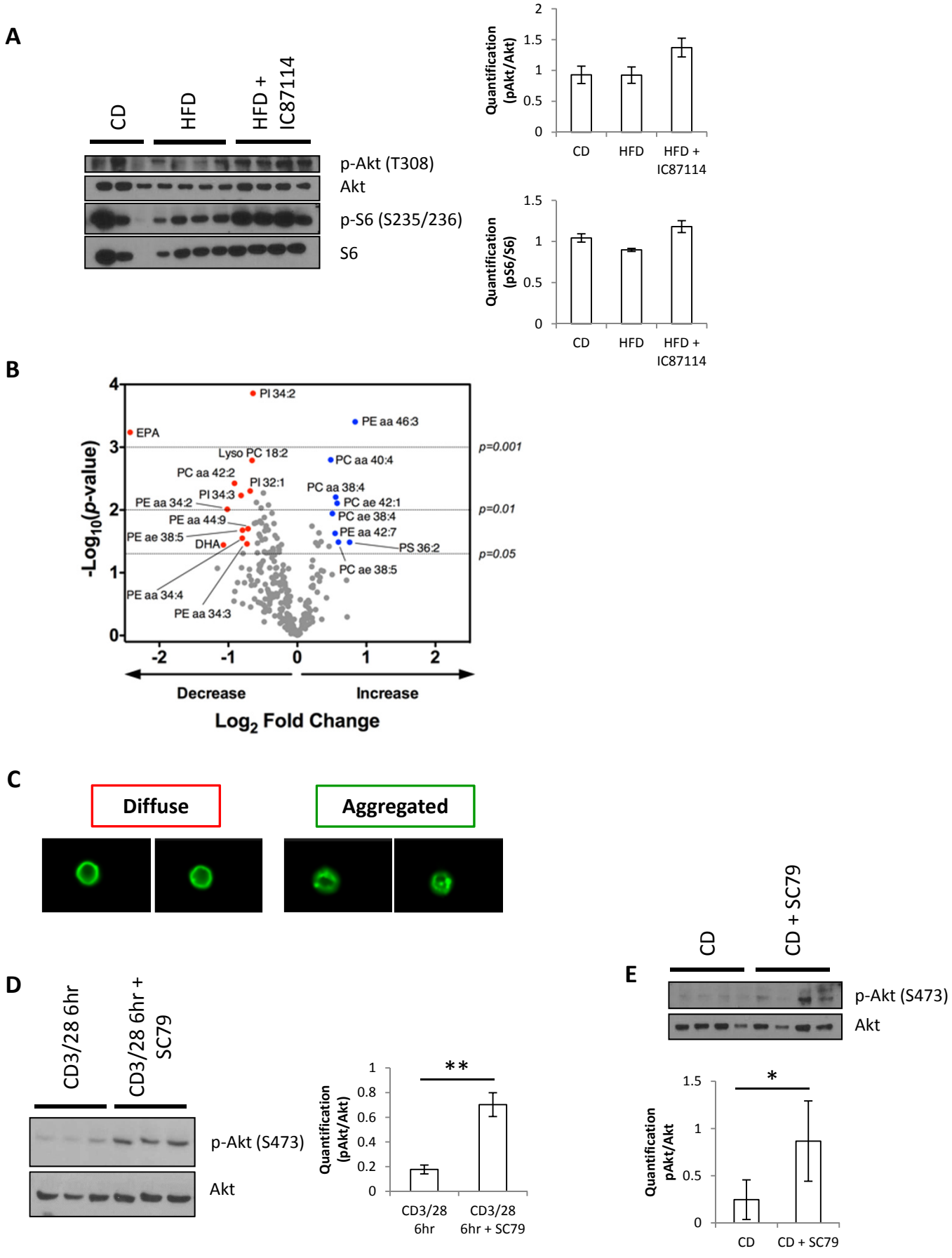

Supplemental Table 1 (related to Figure 3)

	LEAN (N= 370)	OVERWEIGHT (N= 552)	OBESE (N= 250)	P
Age (yrs)	*67 (46-78)*	*68 (52-78)*	*70 (56-78)*	**< 0.001**
Gender (men/women)	*111/259*	*281/271*	*90/160*	
BMI (Kg/m^2)	*22.90 (20.20-24.60)*	*27.10 (25.30-29.10)*	*32.10 (30.40-37.43)*	**< 0.001**
Total cholesterol (mg/dL)	*207.00 (162.00-250.00)*	*201.00 (155.00-250.00)*	*198.00 (151.00-243.00)*	0.279
HDL-C (mg/dL)	*67.00 (48.80-90.00)*	*57 (42-81)*	*57 (40-73)*	**< 0.001**
Triglycerides (mg/dL)	*77 (50-139.4)*	*96 (56-163)*	*99 (64-182)*	**< 0.001**
LDL-C (Friedewald Formula)	*119.2 (81.56-158.8)*	*118.20 (80.92-167.48)*	*118.80 (77.26-158.72)*	0.714
ApoA-I (mg/dL)	*165 (125.8-179)*	*154 (115.7-175)*	*151 (115-174)*	**< 0.001**
Apo-B (mg/dL)	*99 (83-131)*	*101 (79.6-134)*	*99 (81-128)*	0.712
Fasting glucose levels (mg/dL)	*88 (75-104)*	*93 (80-114)*	*100 (84-133)*	**< 0.001**
Total leukocytes (x10^3 U/L)	*5.71 (4.33-8.20)*	*6.36 (4.74-8.80)*	*6.39 (4.71-8.82)*	**< 0.001**
Neutrophils (x10^3 U/L)	*3.31 (2.12-5.12)*	*3.56 (2.43-5.39)*	*3.59 (2.38-5.33)*	**0.010**
Lymphocytes (x10^3 U/L)	*1.78 (1.13-2.55)*	*1.92 (1.36-2.73)*	*1.95 (1.32-2.77)*	**< 0.001**
Monocytes (x10^3 U/L)	*0.49 (0.34-0.75)*	*0.56 (0.39-0.80)*	*0.55 (0.38-0.81)*	**0.002**
Eosinophils (x10^3 U/L)	*0.12 (0.05-0.27)*	*0.15 (0.07-0.33)*	*0.16 (0.07-0.33)*	0.062
Basophils (x10^3 U/L)	*0.03 (0.01-0.05)*	*0.03 (0.01-0.05)*	*0.03 (0.05)*	0.668

Supplemental Table 2 (related to Figures 1, 2 and 4-7)

	High Fat diet (HFD)	**Chow diet (CD)**	**Palmitate-enriched diet (PED)**	**Palmitate-control diet (PCD)**
Fat (%)	***34.9***	***9.1***	***25.2***	***4.2***
Cholesterol, ppm	*301*	*200*	*0*	*0*
Linoleic Acid (%)	*4.7*	*2.32*	*3.86*	*1.89*
Linolenic Acid (%)	*0.39*	*0.21*	*0.29*	*0.29*
Arachidonic Acid (%)	*0.06*	*0.02*	*0*	*0*
Omega-3 Fatty Acids (%)	*0.39*	*0.32*	*0.29*	*0.21*
Total Saturated (%)	*13.68*	*2.72*	*10.05*	*0.39*
Total Mono-saturated (%)	*14*	*2.88*	*10.38*	*1.56*
Polyunsaturated (%)	-	-	*4.38*	*2.07*
Energy (kcal/g)[2]	***5.1***	***3.56***	***4.83***	***3.78***
Protein (%)	*18.1*	*23*	*13*	*16.7*
Fat (%)	*61.6*	*22*	*47*	*10*
Carbohydrate (%)	*20.3*	*55*	*40*	*73.3*